Article

An Urban Flash Flood Alert Tool for Megacities—Application for Manhattan, New York City, USA

Rafea Al-Suhili [1], Cheila Cullen [1,2,*] and Reza Khanbilvardi [1]

[1] Civil Engineering Department, NOAA-Crest Center at the City College of New York, NY 10031, USA; ralsuhili@ccny.cuny.edu (R.A.-S.); khanbilvardi@ccny.cuny.edu (R.K.)

[2] Chemistry, Earth & Environmental Sciences Department, Bronx Community College, CUNY Graduate Center, New York, NY 10479, USA

[*] Correspondence: ccullen@gradcenter.cuny.edu; Tel.: +1-718-289-5569

check for updates

Abstract: Urban flooding is a frequent problem affecting cities all over the world. The problem is more significant now that the climate is changing and urbanization trends are increasing. Various, physical hydrological models such as the Environmental Protection Agency Storm Water Management Model (EPA SWMM), MIKE URBAN-II and others, have been developed to simulate flooding events in cities. However, they require high accuracy mapping and a simulation of the underground storm drainage system. Sadly, this capability is usually not available for older or larger so-called megacities. Other hydrological model types are classified in the semi-physical category, like Cellular Automata (CA), require the incorporation of very fine resolution data. These types of data, in turn, demand massive computer power and time for analysis. Furthermore, available forecasting systems provide a way to determine total rainfall during extreme events, but they do not tell us what areas will be flooded. This work introduces an urban flooding tool that couples a rainfall-runoff model with a flood map database to expedite the alert process and estimate flooded areas. A 0.30-m Lidar Digital Elevation Model (DEM) of the study area (in this case Manhattan, New York City) is divided into 140 sub-basins. Several flood maps for each sub-basin are generated and organized into a database. For any forecasted extreme rainfall event, the rainfall-runoff model predicts the expected runoff volume at different times during the storm interval. The system rapidly searches for the corresponding flood map that delineates the expected flood area. The sensitivity analysis of parameters in the model show that the effect of storm inlet flow head is approximately linear while the effects of the threshold infiltration rate, the number of storm inlets, and the storm inlet flow reduction factor are non-linear. The reduction factor variation is found to exhibit a high non-linearity variation, hence requiring further detailed investigation.

Keywords: urban flooding; flooding map database; urban flash flood alert system; infiltration; storm inlet flow; rainfall-runoff model; digital elevation model

1. Introduction

It is estimated that more than half of the global population currently resides in cities, and it is expected that by the year 2050, at least 66% of the world's population will be urban [1]. The process of urbanization presents significant changes to the natural hydrological paths of an area. By turning natural soil into impervious surfaces (roads, parking lots, buildings, and sidewalks), urbanization reduces rainfall infiltration and decreases runoff time. This in turn significantly alters the peak discharge of storm drainage from the area and usually results in flooding [2].

Urban flooding presents a great challenge for the management of urban water systems, not only because it requires an interdisciplinary approach, but also because flooding in the city usually results in significant human and/or economic losses [3]. For these reasons, urban flash flood warning systems need to quickly forecast which streets and areas will be flooded at any instance during a severe rainstorm. The real-time forecast of areas expected to be flooded within an urban district needs to be quick and easily applicable enough to assist authorities in any decision-making process.

Available flash flood modeling systems can be classified into three broad categories: physical, semi-physical and image processing. Physical systems usually couple meteorological data, overland physical parameters, and the underground sewage flow system [4]. There are various physical models currently available, one of them is the Penn State Urban Runoff Model (PSURM), a system that simulates sewage pipe sizes and uses nonlinear reservoir routing systems to determine flooding. Another system, the MIKE URBAN, was designed from water distribution networks and stormwater systems. Also, the Distributed Routing Rainfall-runoff Model (DR3M-QUAL), a model that incorporates soil moisture, evaporation, pervious and impervious areas amongst other parameters to determine rainfall excess [5]. Nevertheless, these models are dependent on the availability of accurate mapping or simulation of the underground storm drainage systems. The issue is that this type of information usually does not exist, or it is not completely digitized for older or larger cities.

Semi-physical systems like the cellular-automata (CA) approach relies on the cell computation of a discretized space that encompasses a cell state, a time step, and a set of transition rules to other neighboring cells [6]. There are several noteworthy and accessible to the public CA flooding systems such as the Cellular Automata Dual-Drainage Simulation (CADDIES), which couples a series of CA models to simulate surface and subsurface flow [7]; the LISFLOOD-FP model is another CA system that simulates dynamic flood grid cells; the LISFLOOD-FP model also has the capability of assimilating topological information derived from laser or radar [8]. However, the accuracy of these methods depends on the high resolution of time steps and grid cell sizes, these conditions, in turn, require massive CPU parallelism and computer power [6].

Any system that relies on the continuous input of real-time Closed-Circuit Television (CCTV), satellite or radar images are referred to as image processing methods. Such information can assist in characterizing anomalous water level fluctuations. Lo et al. 2015 for example developed an automated remote analysis for monitoring urban floods where CCTV images are automatically monitored to determine flooding areas [9]. In another study, Mason et al. combined Synthetic Aperture Radar (SAR) sensors and Light Detection Ranging (LiDAR) in order to generate map features that can be compared to an electromagnetic scattering model. The image classification system was very successful in differentiating flooded from non-flooded images [10]. Although very successful methodologies, these image-processing methods require either the adaptation of devices such as CCTV equipment, or access to high resolution remotely sensed data, which is in both instances potentially very expensive.

These three types of systems are challenged by either data availability or associated time and expense. Existing rainfall forecasting models also, are challenged as alert systems because they lack the geographical component. They may provide a way to determine the amount of rain during extreme rainfall events, but they do not provide insight into the geographical area expected to be flooded. For these reasons, we propose a system that couples a rainfall-runoff model with a flood map database. Working in conjunction, these two systems can reduce computational time and provide an estimate of flood locality, hence expediting the alert system process.
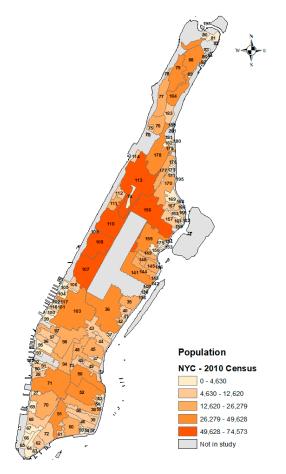
Initially, we take a 0.30-m horizontal resolution Digital Elevation Model (DEM) representation of our area of study, Manhattan, and divide it into 140 sub-basins. For each sub-basin, we remove all building structures so they do not interfere with either our elevation values or our rainfall-runoff model computations. Then, starting at the lowest topographic value and with a step increment, we generate several flood-level maps at each location assuming full routing of the runoff water. All the maps are then assembled into a map database. Consequently, we introduce a rainfall-runoff model that estimates the expected runoff volume at different times during any storm interval.

The model works with the predicted rainfall intensity and duration of any given storm. It simulates rainfall, infiltration, and inlet-flow processes. It also estimates the runoff volume at any time during the storm time interval. With the known runoff volume, the system searches for the map that reflects the flood area. This approach reduces computational time because the database already contains thousands of maps that can reflect how each locality can be affected. If the predicted area is large, authorities can determine whether or not to make changes to local traffic patterns for example. City planners can also potentially benefit from knowing in advance what urban areas are more likely to be flooded. Actions that improve runoff infiltration can be taken at these specific locations, hence reducing the effects of urban flooding.

2. Materials and Methods

In this study, we take Manhattan Island, New York City (NYC) as our megacity area of study. NYC is among the 10 most populated cities in the world [11]. With around 1,664,727 people living in a 59.13 km^2 area [12], Manhattan Island is considered to be the most densely populated city of the United States and the world. It is important to note that this population density does not account for the influx of people commuting into the island every day.

Often described as the cultural and financial capital of the world, Manhattan is host to the United Nations Headquarters, the New York Stock Exchange, and the NASDAQ. Geographically, the East, Harlem and Hudson rivers surround Manhattan, and the city is informally divided into Upper Manhattan, Midtown, and Lower Manhattan. Manhattan averages an elevation of 9.1 m over sea level with the highest point at 81 m, located in Upper Manhattan. The lowest point is located in Downtown Manhattan at 1 m.

Figure 1. Area of study, Manhattan Island NYC—Sub-basins in the study labeled as numbers and corresponding population densities.
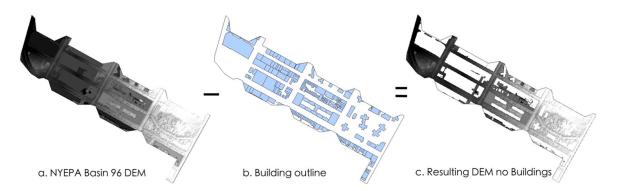
We base this work on the 140-stormwater sub-basins designed by the New York Environmental Protection Agency (NYEPA) [13]. We use a DEM derived from the 2010 Light Detection and Ranging (LiDAR) data at a 0.30-m horizontal resolution with a vertical RMSE between 9.5 cm and 33.08 cm [14]. Figure 1 shows the 140 sub-basins and population densities of each of the areas.

2.1. Flood Map Database

The database is a collection of flood maps for each one of the 140 sub-basins of our study area. This map collection provides a geographical approximation of flooded areas at different rainfall volumes. It also reduces computational time because most possible flooding scenarios have already been pre-prepared.

In order to build this database, we acquired elevation, man-made structures (buildings, streets, sidewalks), and land cover information from the NYC Open Data repository [14]. All data were processed in ArcGIS 10.4 and Python to facilitate automation. We created separate elevation, structures and land cover raster files for each of our sub-basins. In this manner, each sub-basin can be treated as a sub-area of study.

The original DEM contains elevation values of all buildings and structures, but our hydrological analysis is limited to that of the land surfaces other than buildings. Therefore, we subtracted the building footprint for all 140 sub-basin DEM files. We also assumed that the rainwater on the rooftops is collected through the building storm drainage and directly transferred to the stormwater system. Figure 2 depicts a sub-basin DEM before and after building/structure subtraction.

a. NYEPA Basin 96 DEM   b. Building outline   c. Resulting DEM no Buildings

Figure 2. Building outline removal process from DEM file for NYEPA Basin-96—(**a**) Original DEM file with no extractions (**b**) Buildings/structures location within the basin (**c**) Resulting DEM file with no buildings.

We calculated the total sub-basin area A_i; the length of the streets LSi; the land cover types (impervious AI_i, bare soil Ab_i, and green areas Ag_i); and the lowest and highest topographical points in each sub-basin. The approximate number of storm sewer inlets NC_i was derived using Equation (1) below, where S is the spacing between storm inlets in the catch basin and NB is the number of sub-basins in the study area (NB = 140). It is important to note that for our particular area of study, S is based on the NYEPA sewage layout, which includes one inlet at each corner of major intersections and equally spaced inlets along streets. However, we used Equation (1) below to estimate the number of inlets in the area. Then, all information for each sub-basin was transferred to an Excel file.

$$NC_i = \frac{LS_i}{S}, i = 1, 2, \ldots . N_B \tag{1}$$

Starting at the lowest topographic points for each sub-basin DEM file (i), each elevation increment (ΔL) is considered a new flood level Li,j. For example, the lowest DEM topographic pixel point at NYEPA Basin-96 is 2.12 m, this is, $LowL_i$. At an interval ΔL = 15.25 cm, the next level, $LowL_2$, is 2.27 m, $LowL_3$ is 2.42 m, and so on. We calculated flooding volumes (V) and the total flooded area for each flood

level in a new map. In our example above, the total flooded area at $LowL_i = 68.5 \text{ m}^2$, $LowL_2 = 577 \text{ m}^2$, $LowL_3 = 1{,}260 \text{ m}^2$, etc. Equation (2) explains the computations in this process.

$$V_{i,j} = \left[\left[\begin{array}{cc} \sum\limits_{m=1}^{Npi}\left(L_{i,j} - Pl_m\right) * Ap_m & if \; L_{i,j} > Pl_m \\ 0 & otherwise \end{array} \right]\right], \; j = 1, 2, \ldots n \tag{2}$$

where Npi represents the number of pixels in the sub-basin, Pl_m is the pixel level, Ap_m the pixel area, and $L_{i,j} = LowL_i + j\Delta L$, $j = 1, 2 \ldots n$; where $LowL_i$ is the lowest topographic point at sub-basin i, $L_{i,\,j}$.

The final database is then composed of a table of records containing descriptive information about each sub-basin (permeable, not permeable, land cover, etc.), corresponding flood levels, flooded area, runoff volume, and a resultant flood map. The flow chart in Figure 3 shows the complete process implemented for building the database.
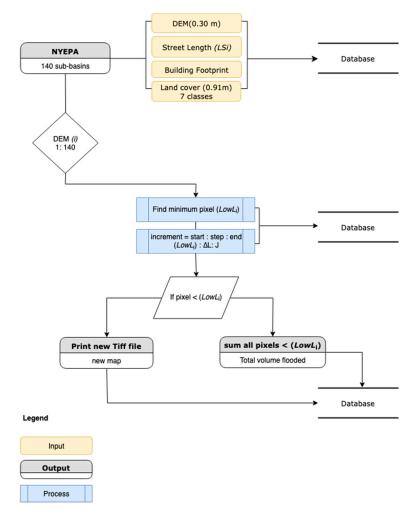

Figure 3. Flow chart describing the process of building the map flood database.

2.2. Rainfall-runoff Model

The rainfall-runoff model presented here follows the concept of mass balance in a catchment area and includes physical processes of rainfall, infiltration, and storm inlet flow. Here, this concept is applied to each pixel of the DEM raster. The volume of rainfall received at each pixel within a time period represents the inputs. The outflows are represented by infiltration and street inlet flows but exclude evaporation. Input and outflows are subtracted to determine the remaining flooding volume

at the end of the storm period. The total flooding volume for the area is the sum of the runoff volume for all pixels.

The use of pixel-based mass balance allows for temporal and spatial rainfall intensity variations. It also allows for infiltration differentiation according to land cover type. For pixels containing inlets, we determined storm street inlet flow by incorporating Armal and Al-Suhili 2019 [15] proposed methodology. This methodology accounts for inlet blockages and it is explained below. In addition, we used Horton's infiltration model to determine the time effect from initial infiltration until threshold rate.

The innovative approach presented here relies on the coupling of the model and the flood map database. The flood maps are easily accessible throughout the storm event as well as during the recession period. We implemented the following steps for the creation of model:

(1) For any expected rainfall event, the total period of storm T and its rainfall intensity (I_t) time variation is shown on the storm hyetograph in Figure 4.
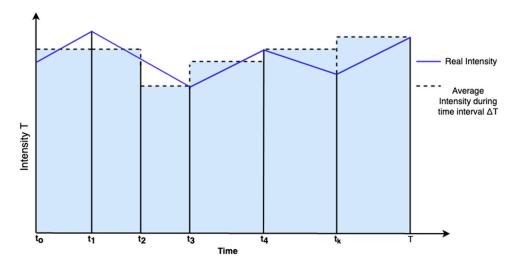

Figure 4. Hyetograph for actual and average rainfall intensity during time interval.

(2) The user selects time interval ΔT, which in turn selects the number of time steps N_T and flood maps as per Equation (3).

$$N_T = \frac{T}{\Delta T} \tag{3}$$

Maps are displayed for each time interval as shown in Equation (4).

$$t_k = k\Delta T, k = 1, 2, \ldots .N_T \tag{4}$$

where t_k represents time from the beginning of the storm event up to k intervals of ΔT.

The flooding event simulation can be extended to cover the storm recession period (i.e., the period after the rainstorm ends, up to the time where the runoff water is fully drained by the storm sewer network). In this case, Equation (4) is extended as follows:

$$t_k = k\Delta T, k = 1, 2, \ldots ..(N_T + N_R) \tag{5}$$

where, N_R is the number of time steps ΔT, for the recession period, i.e., after the rain stops, as selected by the user.

(3) The rainfall intensity during any period, t_k *to* t_{k-1} is obtained by averaging the intensities at those times. The following equation can be used for the rainfall intensity during the total time of the storm event and recession period.

$$R_k = \left[\begin{array}{cc} \frac{I_{t_k}+I_{t_{k-1}}}{2} & k = 1,2,3,\ldots.N_T \\ 0 & k > N_T, \; and \; k < (N_T + N_R) \end{array} \right]$$

(6)

where R_k is the average intensity over time (t_k, t_{k-1}).

(4) Using rainfall, infiltration and the storm inlet flow processes, runoff volume at any time t_k is estimated using the following equation:

$$V_k = V_{k-1} + R_k A_i - Inf_k - D_k k = 1,2,\ldots N_T$$

(7)

where V_k, and V_{k-1} are runoff volumes at time intervals t_k and t_{k-1} respectively, D_k represents the volume of water drained through the street inlets of the storm sewer system during time interval ΔT, as per Liu et al. 2015 [16], and Inf_k represents the infiltrated volume during the time interval as:

$$Inf_k = \Delta T \left(A_b . f_b + A_g . f_g \right)$$

(8)

where f_b and f_g are the average infiltration rates for bare soils and green areas.

The equation below is used for calculating the inlet flow as water intake rate:

$$Q = k.w.C \sqrt{2gh}$$

(9)

In order to simulate inlet flow partial blockage, and its resulting backflow, we modified Equation (9) into Equation (10) by introducing the β factor as proposed in Armal and Al-Suhili 2019 [15]. Here, β fluctuates between −1 and 1 during the simulation time interval. 1 represents a full inlet, at full inlet inflow capacity. A partial blockage results in a number between (1 and 0). 0 represents a full blockage, and values between (−1 and 0) represent a partial backflow while a value of −1 represents full backflow. A linear beta-time variation is assumed with negative trend (slope) and an initial value of 1, (i.e., beta decreases from 1 to −1 with time). The slope value is first assigned according to the topography of the area and the location of the inlet. We verified the assigned slope value using the head variation with time in the pixels that include an inlet. We assumed that the inlet starts back flowing when there is an increase on the head (flood depth) that is not related to the amount of rainfall.

$$Q = \beta \, k.w.C \sqrt{2gh}$$

(10)

where Q is the inlet discharge flow $m^3 s^{-1}$, w is the area of the inlet m^2 C represents the orifice coefficient, g is the gravitational acceleration, h is the allowed water storage head of an inlet, and k is orifice obstruction coefficient to account for interception of outlet screen racks. With this equation, then we can estimate the inlet volume D:

$$D_k = \Delta T(Q)(NC_i)$$

(11)

(5) The simulation starts by setting the initial runoff volume, i.e., at t = 0, as V_0 = 0. The system proceeds to estimate V_k for different k-values. Then, at each appraised volume, the model calls the map database and displays the map that closely matches the projected runoff volume.

The rainfall-runoff model simulation process uses the above calculations at selected time intervals during the storm. Infiltration rates are determined using Equation (12), Horton's equation. The storm sewer inlets are determined using Equation (10). The initial value of β is 1, and it is assumed to reduce with time during the simulation period. A negative β value is adopted if the total storm interval lasts long enough to produce backflow. The inlet flow head, h, is assumed to increase linearly with time. Accuracy of the simulation is, of course, affected by time variations of these factors. The actual and the simulated runoff depths are expected to have small differences, but they do not affect our objective of pre-identifying flood areas. The expected damages and consequences of severe floods, i.e., 40 cm or higher, will not be much affected by a few centimeters of flood depth.

3. Results

In this work, the sub-basin database and the rainfall-runoff model work together to reduce computational time and provide a map of the flood area. The database informs the model about the specific conditions (paved areas, permeable areas, land cover type, total area, etc.) of each sub-basin and subsequently delivers the appropriate flood map of the area.

In the following pages, we assess the capability of the rainfall-runoff model to forecast flooding areas in an extreme rainfall event. We evaluate the efficacy of the pre-prepared database in relation to the rainfall-runoff model and its capability to select the best suitable flood map and last, we apply the system functionality to a case study in the area.
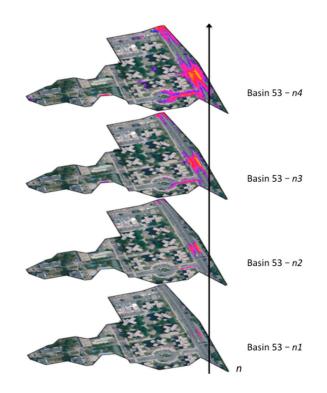
3.1. Database

The full assembly of the database results in a set of tabulated information as shown in Table 1 and a set of corresponding maps as shown in Figure 5.

Table 1. Tabulated information for each basin connected to a corresponding map.

Flooded Volume m^3	Roads	Paved Other	** Bldg.	Bare	Grass/ Shrub	Tree Canopy	Total *** P.A.	Total Area	Population	Basin ID Level
2598	152	0	0	0	0	14.7	14.7	257,900	2263	Basin 53-n1
20,889	996	28	0	0	9.1	204	213	257,900	2263	Basin 53-n2
72,921	2525	378	0	0	27.4	1132	1159	257,900	2263	Basin 53-n3
209,073	5657	1460	156	0	75.9	3615	3691	257,900	2263	Basin 53-n4
427,873	8513	3843	302	0	243	8265	8526	257,900	2263	Basin 53-n5
…	…	…	…	…	…	…	…	…	…	Basin 53-n...

* All units in m^2 unless specified—** Buildings. *** Permeable Area.

Figure 5 below shows four levels corresponding to basin number 53 located on the lower East side of Manhattan, each one of these maps corresponds to the first four rows of information in Table 1.

Figure 5. Flood levels for NYEPA Basin number 53 where n represents each new flood level at subsequent elevation ΔL increments.

As the user selects the sub-basin of interest and inputs the expected amount of rainfall and it's duration, several maps in pdf format are displayed or printed for the area as shown in Figure 6 below.

Figure 6. Expected flooded area (EFA) for base level (Lowli) and subsequent ΔL = 15.25cm increments Basin53—(**a**) Lowest topographic level—Lowl1 = 1.62 m, EFA = 500 m^2; (**b**) Lowl2 = 1.77 m, EFA = 3745 m^2; (**c**) Lowl3 = 1.92 m, EFA = 12,228 m^2; (**d**) Lowl4 = 2.08 m, EFA = 32,834 m^2; (**e**) Lowl5 = 2.23 m, EFA = 63,649 m^2; (**f**) Lowl6 = 2.39 m, EFA = 102,251 m^2.

3.2. Case Study—Extreme Rainfall Event May 5, 2017

The May 05, 2017 storm and the corresponding flood that affected Manhattan Island, NY, is used as a case study for the model. The estimated average intensity of the storm was 15.3 cm/hour. This averaged intensity is distributed over a 15-min duration. The specific sub-basin location in Manhattan is identified as Basin-96 in the NYEPA designation. The basin encompasses the area between 12th Avenue in the West, 8th Avenue in the East, 23st in the South and 26st in the North. Figure 7 below shows the total basin area.

Figure 7. Case study area—NYEPA Basin 96—12th Avenue in the West, 8th Avenue in the East, 23st in the South and 26st in the North.

The basin total area is 244,713 m^2, the pervious area is 15,623 m^2, and the total street length is 5124 m. The soil type of this area indicates the following Horton's infiltration parameters for the application of time variant infiltration rate: fo = 0.1423 cm/min, ff = 0.0021 cm/min, and k = 0.07 1/min.

$$f_t = f_f + \left(f_0 - f_f\right)e^{-kt} \tag{12}$$

where $f_t(mm/h)$ is the infiltration rate at time t; $f_0(mm/h)$ is the initial infiltration capacity, $f_f(mm/h)$ is the final infiltration (threshold value) capacity, k is the decay constant, and t is time. There are 34 estimated storm sewer inlets in the basin. The head of each inlet is assumed to be 0.05 m at the start of the storm and increase at a linear rate to a threshold value of 0.1 m. The inlet flow was deduced using the reduction factor *β* as mentioned above. With this information, the model application resulted in the outputs shown in Table 2 below.
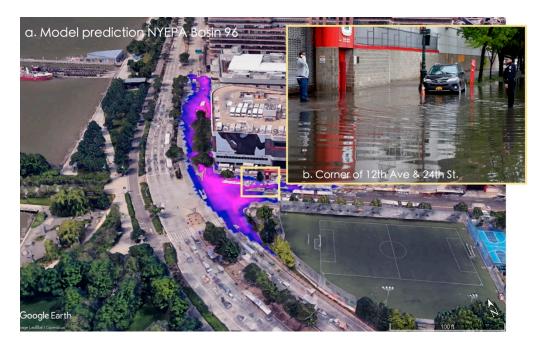
Table 2. Rainfall-runoff model results.

TIM *	Accumulated Runoff Volume at the Beginning of Interval—m^3	Rainfall Volume m^3 During the Interval	Infiltration Rate cm/min During the Interval	Infiltrated Volume m^3 During the Interval	Reduced Factor IDC **	Inlet Head	Drained Volume SSS *** During the Interval	Accumulated Runoff Volume at the End of Interval m^3
0–5	0	3108	0.076	279.8	0.34	0.05	1717	1110
5–10	1110	3108	0.055	201.5	0.27	0.07	1673	2343
10–15	2343	3108	0.049	178.8	0.20	0.10	1428	3843

* TIM (Time interval in minutes), ** IDC (Inlet discharge coefficient), *** SSS (storm sewer system).

The model searches the database to find the closest flooding map that represents the actual runoff volume. For our case study, Figure 8a. shows the map corresponding to the rainfall event. A picture of the corner of 24th St and 12th Avenue (area within NYEPA Basin 96) shows actual flooding during

the May 5th storm in Figure 8b. This area corresponds to the West Side Highway (12th Avenue), a major transportation way in Manhattan. As reported by numerous media outlets [17,18] the heavy downpour caused several road closures around the metropolitan area. The National Weather Service reported closures between 20th and 30th streets on the West Side Highway at around 1:40 PM due to flooding [19].

Figure 8. (**a**) Model Prediction for May 5, 2017 in NYEPA Basin 96—Extreme flooding event for 12th Avenue between 24th and 25th streets (**b**) Flooding image taken on May 5, 2017 at the corner of 12th Avenue and 24rd street (Carlo Allegri, Reuters).

The study case shows that the system can generate several flood level maps that are congruent with actual flooding. The picture taken of the flooded area at the moment after the storm coincides with the area assigned as flooded by the model. The case study also shows that the system is consistent with mass conservation at reasonable computational time.

As the average intensity of the storm is an estimate, its value may impact the model's precision. Nevertheless, since our goal is to quickly determine the area that is most likely to be flooded, the system rapidly computes volumes and chooses the corresponding flood map. Results for this case study show that for a 15-min storm period, subdivided at 5-min intervals, the total computational time is 3 min.

3.3. Parameter Sensitivity Analysis

Sensitivity analysis is useful for finding the percentage change variation in the estimated volume. It helps us define the level of accuracy required for setting temporal and spatial variations of parameters in the model. Specifically, to detect whether their variation is linear or non-linear and if these changes are relatively high or low.

Table 3 below shows percentage reductions in runoff volume at the end of the storm due to variations of different parameters.

Table 3. Runoff volume reduction as percentages.

Inlet Head Effect	Reference Value	Storm Inlet Head-Time Variation cm/Time Interval	Runoff Value Percent Reduction—from Reference	Runoff Value Percent Reduction—from Previous
	0.01	0.01	0	0
		0.015	3.47	3.47
		0.02	6.76	3.41
		0.025	9.91	3.37
Threshold Infiltration Rate Effect	Reference Value	Threshold Infiltration Rate	Runoff Value Percent Reduction—from Reference	Runoff Value Percent Reduction—from Previous
	0.048	0.048	0	0
		0.04	−0.76	−0.76
		0.032	−1.46	−0.69
		0.26	−1.98	−0.52
Number of Inlets Effect	Reference Value	Number of Inlets variation	Runoff Value Percent Reduction—from Reference	Runoff Value Percent Reduction—from Previous
	34	34	0	0
		32	−6.25	−6.25
		30	−12.49	−5.88
		28	−18.74	−5.55
Sewer Inlet Flow Coefficient Effect	Reference Value	Variation Change Per Time Interval	Runoff Value Percent Reduction—from Reference	Runoff Value Percent Reduction—from Previous
	0.06	0.06	0	0
		0.04	11.17	11.17
		0.02	19.49	9.37
		0	27.82	8.33

Parameter sensitivity analysis showed the following. With respect to the low head time variation for the storm inlets, the change in head variation was set at 0.01 cm/min as reference value and time interval was set at 5-min. We tried different variations at 0.015, 0.02 and 0.025 cm/min. Results showed an approximate linear variation at a rate of approximately 3.4 percent increase. Regarding variation of the threshold infiltration rate, the reference value was set to 0.048 cm/min and it was reduced to 0.04, 0.032 and 0.26 cm/min. The time interval was also set at 5-min. Results indicated a non-linear variation of runoff flow with a small (0.76 to 0.52) percent increase. With respect to the effect of the number of storm inlets, we used 34 as reference value and reduced it by 2 at each 5-min interval. We also observed a non-linear variation in this parameter. The percentage increase in runoff flow ranged between 6.25% and 5.55%. Finally, concerning the storm inlet flow reduction factor effect, time variation was found to be non-linear with a range between 11.7 and 8.33. This indicates that variations of this parameter are very sensitive and need further investigation for future applications.

4. Discussion

This paper introduces a coupled GIS-based model and map database that simultaneously works to facilitate the urban flooding management process. The purpose of this coupling is so that potential flooded geographically areas can be determined before the storm. Given the complexity of all model types (physical, semi-physical, image processing, etc.), this approach was developed with some simplified assumptions. Evaporation, for example, is not considered as a variable in the model since its value during a storm event is not significant.

We underline that various assumptions and variations of the many parameters in the model will affect accuracy. The accuracy of inundation depths in this model for example, relies solely on the calculation of the rainfall amount, infiltration rate, and the storm inlet flow processes. In addition, the extent of the flooded area is considered to decrease with distance from the maximum head or

inundation depth. Nevertheless, we achieve our objective to present a system that can quickly simulate flooded areas before the storm.

Our study case demonstrates that computational time is relatively short. The system took 3 min to complete calculations for three time intervals of a 15-min storm. We also tried five different intervals, at 3 min each, for a 15-min storm. The system completed all the calculations in 4 min. The interval time and the processing time are not linearly correlated, but overall, compared to other available systems, this model can be used as a quick reference.

4.1. Limitations

(1) Verification limitations: depth verification is not presented in this document and is needed for future fine-tuning of the model. At this time, the model is devoted to finding areas prone to urban flooding and their extent.

(2) Homogeneous rainfall: as spatial variations of rainfall must be considered, the system here presented is completely reliant on the availability of detailed rainfall forecasts and rain gauges.

(3) Temporal rainfall distribution: the rainfall time-intensity variation is not considered, and consistent average rainfall intensity is assumed during the storm time interval.

(4) Data limitations: the presented model is a data driven system that relies on the accuracy of data inputs. In this case, we have used a 0.30 m resolution LiDAR DEM of NYC but other relevant information such as land use and land cover types are not yet available at such resolution.

(5) Sub-basin-based inundation: in this study, flooding is calculated separately for each sub-basin. Uneven or unrealistic flooding conditions may be encountered at each sub-basin boundary area.

(6) River flooding: based on the limitations and criteria that the system is built on, the system is not appropriate to use for river flooding.

4.2. Future Directions

Validation with a future rainfall event needs to be studied to compare model results to real flood depth spatial distribution. Furthermore, as sensitivity analysis demonstrates, the reduction factor variation needs further analysis as it exhibited a high non-linear variability. As we fine-tune the system, it will be extended to the other boroughs of New York City.

5. Conclusions

We propose an urban flash flood alert tool that couples a rainfall-runoff model with a flood-level map database that expedites the alert system process. The pre-prepared flood maps database can be used for a quick identification of the areas prone to flooding when coupled with the rainfall-runoff model, with very short processing computer time compared to other models. Our approach presents reasonable flooding results for the sake of quick preparedness. We expect that the resultant maps can inform authorities and citizens about expected conditions in the streets and on the roads in the city as a storm approaches. It is our hope that decisions, such as closing traffic in a particular area, can be aided by this system.

The spatial flood depth distribution of the flooded area can be estimated at any time within the storm interval using ArcGIS. Unfortunately, this flood runoff depth spatial distribution cannot be verified due to the lack of spatial depth measurements during the storm event of the case study, and hence left for future research. As for the current document, the objective is only to develop a model for identifying areas prone to flooding and the extent of the flood regardless of the depth, i.e., any area covered by residual water.

Sensitivity analysis of the model showed that the storm inlet flow parameter exhibits a linear variation of (3.4%). The threshold infiltration rate, the number of storm inlets and the storm inlet reduction factor showed a non-linear variation. However, the reduction factor variation showed a high non-linear variation, as it is a very sensitive parameter. For this reason it is necessary to further research

the effects of this factor in relation to the overall model. Perhaps in the future, with the acquisition of real-time depth data from satellites, this factor can be calculated with more precision.

Lastly, in spite of the limitations posed by the rainfall spatial and temporal variations, the model was developed in such a way that these variables could easily be included using GIS-Excel data files in future work.

References

1. Population Division, Department of Economic and Social Affairs, United Nations. *World Urbanization Prospects*; United Nations: New York, NY, USA, 2014; p. 32.
2. NRCS. *Urban Hydrology for Small Watersheds TR-55*; Technical Release 55; United States Department of Agriculture: Washington, DC, USA, 1986; p. 164.
3. Ahmad, S.S.; Simonovic, S.P. Spatial and temporal analysis of urban flood risk assessment. *Urban Water J.* **2013**, *10*, 26–49. [CrossRef]
4. Pina, R.D.; Ochoa-Rodriguez, S.; Simões, N.E.; Mijic, A.; Marques, A.S.; Maksimović, Č. Semi- vs. Fully-distributed urban stormwater models: Model set up and comparison with two real case studies. *Water* **2016**, *8*, 2. [CrossRef]
5. Rangari, V.A.; Patel, A.K.; Umamahesh, N.V. Review of Urban stormwater Models. *Environ. Model. Softw.* **2000**, *16*, 37.
6. Guidolin, M.; Chen, A.S.; Ghimire, B.; Keedwell, E.C.; Djordjević, S.; Savić, D.A. A weighted cellular automata 2D inundation model for rapid flood analysis. *Environ. Model. Softw.* **2016**, *84*, 378–394. [CrossRef]
7. U. AC CADDIES. 2015. Available online: http://emps.exeter.ac.uk/engineering/research/cws/resources/caddies-framework/ (accessed on 21 March 2018).
8. LISFLOOD-FP. Available online: http://www.bristol.ac.uk/geography/research/hydrology/models/lisflood/ (accessed on 21 March 2018).
9. Lo, S.W.; Wu, J.H.; Lin, F.P.; Hsu, C.H. Visual sensing for urban flood monitoring. *Sensors* **2015**, *15*, 20006–20029. [CrossRef] [PubMed]
10. Mason, D.C.; Giustarini, L.; Garcia-Pintado, J.; Cloke, H.L. Detection of flooded urban areas in high resolution Synthetic Aperture Radar images using double scattering. *Int. J. Appl. Earth Obs. Geoinf.* **2014**, *28*, 150–159. [CrossRef]
11. United States Census Bureau. United States Census Bureau, Quick Facts. 2017. Available online: https://www.census.gov/quickfacts/fact/table/newyorkcountymanhattanboroughnewyork,US/PST045217 (accessed on 10 October 2018).
12. New York State, GIS.NY.GOV. 2018. Available online: https://gis.ny.gov/gisdata/inventories/member.cfm?organizationID=529 (accessed on 10 October 2018).
13. NYC Open Data. 2010. Available online: https://opendata.cityofnewyork.us/data/ (accessed on 10 June 2018).
14. NYC Open Data. 2010. Available online: https://data.cityofnewyork.us/browse?q=DEM (accessed on 12 January 2018).
15. Armal, S.; Al-Suhili, R.; Khanvilbardi, R. An Urban Flood Inundation Model Based on Cellular Automata. *Int. J. Water* **2019**, 20.

16. Liu, L.; Liu, Y.; Wang, X.; Yu, D.; Liu, K.; Huang, H.; Hu, G. Developing an effective 2-D urban flood inundation model for city emergency management based on cellular automata. *Nat. Hazards Earth Syst. Sci.* **2015**, *15*, 381–391. [CrossRef]

17. Heavy Rain in New York Causes Flooding, Road Closures, Daily News. 2017. Available online: https://www.nydailynews.com/new-york/heavy-rain-new-york-city-flooding-road-closures-gallery-1.3140329 (accessed on 16 November 2018).

18. Rosenberg, E. Flooding in New York shuts down roads and strands drivers, New York Times. 2017. Available online: https://www.nytimes.com/2017/05/05/nyregion/flooding-new-york-roads-shutdown-rain.html (accessed on 16 November 2018).

19. National Weather Service. May 5th Flash Flood Event. Weather.gov. Available online: https://www.weather.gov/okx/storm05052017 (accessed on 15 November 2018).